TRANSITIONS IN THE SOLVATION STRUCTURE ABOUT IONS IN SUPERCRITICAL WATER AND THEIR EFFECTS ON REACTIVITY

John L. Fulton, Markus M. Hoffmann, John G. Darab
Pacific Northwest National Laboratory,
P.O. Box 999 MS P8-19
Richland, WA, 99352.

ABSTRACT

We have determined the molecular structure about ions in water under hydrothermal conditions using X-ray absorption fine structure spectroscopy (XAFS). We report a large decrease in the extent of ion hydration in Ni^{2+}, Sr^{2+}, Rb^{+}, and Br^{-} solutions and the formation of contact-ion pairs in aqueous nickel bromide at temperatures exceeding 325°C. The results demonstrate the large changes in the solvation dynamics that occur in the transition from ambient to supercritical conditions. Such fundamental structural information on the speciation in aqueous solutions under hydrothermal conditions is scarce but needed for an understanding of both inorganic and organic reactions in a supercritical-water solvent. Such an understanding will further the development of new hydrothermal technologies such as organic synthesis or waste destruction processes.

INTRODUCTION

It is well known that ionic species start to associate with their respective counter ions in water at high temperatures. For solutions containing ionic species at moderate concentrations, the onset of this phenomena occurs at temperatures above about 325°C where the breakdown of the water hydrogen-bonding network[1] leads to a dielectric constant (low-frequency) that is dramatically lower than for ambient conditions. The low value of the dielectric constant means that the electrostatic interactions between charged species is no longer effectively screened. A detailed description of the ion-pairing phenomena was first made available through theoretical and simulation work[2,3]. Some experimental evidence[4,5] of the existence of ion-pairing was also derived from electronic and Raman spectroscopy but yielded little direct structural information. This XAFS technique[6-9] gives the short-range structure of the first several solvation shells about the ion. Therefore, for the first time, we can measure the detailed structural transitions that occur under hydrothermal conditions. We have previously reported observation of significant dehydration occurring under supercritical water conditions for mono- and di-valent cations[10-12] (Sr^{2+} and Rb^{+}) and for a monovalent anion (Br^{-}).[13] More recently we have explored $NiBr_2$ hydration and ion pairing in moderately dilute systems.[14] Seward et al.[15] have also reported XAFS studies of the hydration and ion-pairing of Ag^{+} in subcritical water solutions at their vapor pressure. In this paper, we explore a Ni^{2+} system in which the Br^{-} concentration is greatly increased through the addition of NaBr. This promotes the formation of the more highly coordinated $NiBr_n$ species.

Although this presentation will deal with association of inorganic ions ins supercritical water (T_c = 375°C), the results are important to systems that also contain organic species. The structural transition that occurs for these inorganic species will also have their analogous transition for organic ionic species. Thus, the existence of ion pairs is an important consideration for manipulating reaction pathways and reaction rates in supercritical water. For instance, ion-pair formation may enhance the reactivity of charged organic molecules if it involves the association of two ionic reactant species (oppositely charged) or it involves an ionic reactant species with an ionic catalytic species. The reactivity may be reduced in those instances where an ionic reactant is sequestered by ion-pair formation with a non-reactive ionic species. Similar mechanisms of enhanced or reduced reaction rates would also affect pathways that involve ionic transition-state species. Finally, the regioselectivity may also be influenced for charged or very polar reactants since the reactants can assume a strongly-bound spatial orientation in an ion-pair structure. It is in this light, that we explore the detailed nature of ion pairing under hydrothermal conditions.

EXPERIMENTAL

In XAFS, the x-ray energy is tuned to the region bounding the electron absorption (in this case the K-edge). The ejected photoelectons are back-scattered by atoms in the nearest solvation shells giving rise to oscillations in the XAFS spectra on the high energy side of the edge. The Fourier transformation of these *k*-space spectra gives a real-space distribution plot that is closely

related to a radial distribution function. XAFS is a short-range technique, that gives structural information out to one or two solvent shells from the central scattering atom. This is the region of critical importance for understanding ion hydration in a water environment. XAFS spectra were acquired at the insertion device beamline (PNC-CAT) at the Advance Photon Source (Argonne National Laboratory) and at beamline X-19A of the National Synchrotron Light Source (NSLS) at the Brookhaven National Laboratory. A schematic of the high-temperature, high-pressure XAFS equipment and of the data transformation methods are depicted in Figure 1. The details of the experimental techniques [11-13,16,17] are given elsewhere.

The methods for data collection, background correction and data transformation are well-established[9,18,19] The analysis of the $\chi(k)$ function was based upon the standard XAFS relationship

$$\chi(k) = \frac{F(k)S_0^2 N}{kR^2} e^{-2k^2\sigma^2} e^{-2R/\lambda(k)} \sin(2kR + \delta(k) - \frac{4}{3}k^3 C_3) \qquad (1)$$

Where $F(k)$, $\delta(k)$, and $\lambda(k)$ are the amplitude, phase and mean-free path factor, respectively, that are derived from the theoretical standard FEFF.[20] Detailed description of fitting methods for these parameters can be found elsewhere.[14] The remaining terms in Equation 1 are N, the coordination number of the shell, R, the shell distance, σ^2, the Debye-Waller factor which represents the mean-square variation in R due to both static and thermal disorder, and finally C_3, the anharmonicity of the pair-distribution. These terms, which contain the quantitative structural information, were found using the FEFFIT[21,22] analysis program that employs a non-linear, least-squares fit to the theoretical standards calculated by FEFF.[20]

DISCUSSION AND CONCLUSIONS

Figure 2 is a radial structure plot for Ni^{2+}. The figure relates the probability of finding a water molecule or a Br^- at some distance from the central Ni^{2+} ion. Under ambient conditions the Ni^{2+} is octahedrally coordinated with 6 water molecules. As the temperature of the solution is increased, the number of water molecules in the first solvation shell decreases and we observe the appearance of a new peak at about 2.1 Å due to the Br^- counterion. In all the systems that have been studied in detail thus far, the decrease in the extent of hydration occurs concurrent with the formation of the contact ion pairs. This may be primarily a size-exclusion effect or may be in part due to the reduction in the local electric field due to the presence of the counterions.

Table 1 relates the change in the extent of hydration upon going from ambient to a supercritical state for a variety of different cations and an anion. Again there are dramatic reductions in the extent of hydration upon reaching supercritical conditions for these ionic species.

Table 2 reports the detailed structural parameters for a $NiBr_2$ contact ion pair. The results are derived from a global-model fit to two independent XAFS measurements at both the Ni and Br absorption edges. Thus, a very high degree of confidence is obtained for the $NiBr_n$ ion-pair structural parameters. In this system, the concentration of the Br^- was increased to 6 times the Ni^{2+} concentration in order to favor the formation of Ni^{2+} species with a high degree of ion pairing. The results strongly suggest that there is a transition from octahedral Ni^{2+} coordination at room temperature to tetrahedral coordination at elevated temperatures. The *average* number of Br^- ions in contact with a Ni^{2+} ion is 3.3. Since electrostatically neutral species are strongly favored in this solvent, the likely species may include dimers $(NiBr_4Ni(H_2O)_n)^0$ or species that also include Na^{1+} association such as $(NiBr_3Na(H_2O)_n)^0$.

In conclusion, a great deal of structural information is available from XAFS about a wide range of supercritical water systems. Information from these studies will aid in the development of structurally-appropriate models of reaction rates and pathways under hydrothermal conditions.

ACKNOWLEDGMENTS

This research was supported by the Director, Office of Energy Research, Office of Basic Energy Sciences, Chemical Sciences Division of the U. S. Department of Energy, under contract DE-AC06-76RLO 1830.

REFERENCES

1. Hoffmann, M. M.; Conradi, M. S. *J. Am. Chem. Soc.* **1997**, *119* 3811-3817.
2. Chialvo, A. A.; Cummings, P. T.; Cochran, H. D.; Simonson, J. M.; Mesmer, R. E. *J.*

Chem. Phys. **1995**, *103*9379-9387.
3. Oelkers, E. H.; Helgeson, H. C. *Science* **1993**, *261*888-891.
4. Susak, N. J.; Crerar, D. A. *Geochim. Cosmochim. Acta* **1985**, *49*555-564.
5. Spohn, P. D.; Brill, T. B. *J. Phys. Chem.* **1989**, *93*6224-6231.
6. Sayers, D. E.; Stern, E. A.; Lytle, F. W. *Phys. Rev. Lett.* **1971**, *27*1204.
7. Lee, P. A.; Citrin, P. H.; Eisenberger, P.; Kincaid, B. M. *Rev. Modern Physics* **1981**, *53*769-806.
8. Lytle, F. W. In *Applications of Synchrotron Radiation*; Winick, H.; Xian, D.; Ye, M.; Huang, T., Eds.; Gordon and Breach: New York, 1989; pp 135-223.
9. Teo, B. K. *EXAFS: Basic Principles and Data Analysis*; Springer-Verlag: New York, 1986.
10. Palmer, B. J.; Pfund, D. M.; Fulton, J. L. *J. Phys. Chem.* **1996**, *100*13393-13398.
11. Fulton, J. L.; Pfund, D. M.; Wallen, S. L.; Newville, M.; Stern, E. A.; Ma, Y. *J. Chem. Phys.* **1996**, *105*2161-2166.
12. Pfund, D. M.; Darab, J. G.; Fulton, J. L.; Ma, Y. *J. Phys. Chem.* **1994**, *98*13102-13107.
13. Wallen, S. L.; Palmer, B. J.; Pfund, D. M.; Fulton, J. L.; Newville, M.; Ma, Y.; Stern, E. A. *J. Phys. Chem. A* **1997**, *101*9632-9640.
14. Wallen, S. L.; Palmer, B. J.; Fulton, J. L. *J. Chem. Phys.* **1998**, *108*4039-4046.
15. Seward, T. M.; Henderson, C. M. B.; Charnock, J. M.; Dobson, B. R. *Geochim. Cosmochim. Acta* **1996**, *60*2273-2282.
16. Fulton, J. L.; Pfund, D. M.; Ma, Y. *Rev. Sci. Instrum.* **1996**, *67(CD-ROM Issue)*1-5.
17. Hoffmann, M. M.; Darab, J. G.; Heald, S. M.; Yonker, C. R.; Fulton, J. L. *Chemical Geology* **1999**, Submitted.
18. Stern, E. A.; Heald, S. In *Handbook of Synchrotron Radiation*; Eastman, D. E.; Farge, Y.; Koch, E. E., Eds.; North Holland: Amsterdam, 1983.
19. *X-Ray Absorption: Principles, Applications, Techniques of EXAFS, SEXAFS and XANES*; Koningsberger, D. C.; Prins, R., Eds.; John Wiley & Sons: New York, 1988.
20. Zabinsky, S. I.; Rehr, J. J.; Ankudinov, A.; Albers, R. C.; Eller, M. J. *Phys. Rev. B.* **1995**, *52*2995-3009.
21. Newville, M.; Ravel, R.; Haskel, D.; Rehr, J. J.; Stern, E. A.; Yacoby, Y. *Physica B* **1995**, *208 & 209*154-156.
22. Stern, E. A.; Newville, M.; Ravel, B.; Yacoby, Y.; Haskel, D. *Physica B* **1995**, *208 & 209*117-120.

FIGURES AND TABLES

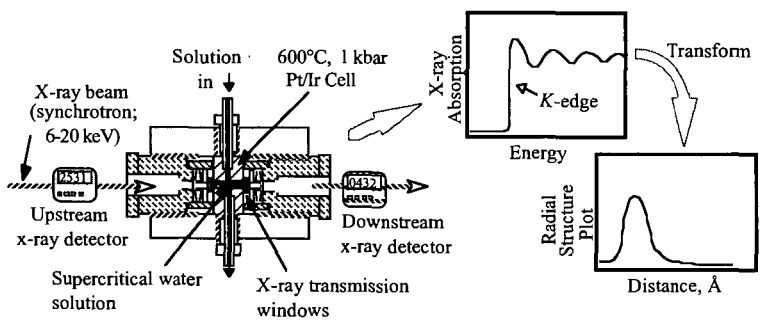

Figure 1. Schematic of the supercritical water XAFS cell and the data analysis technique.

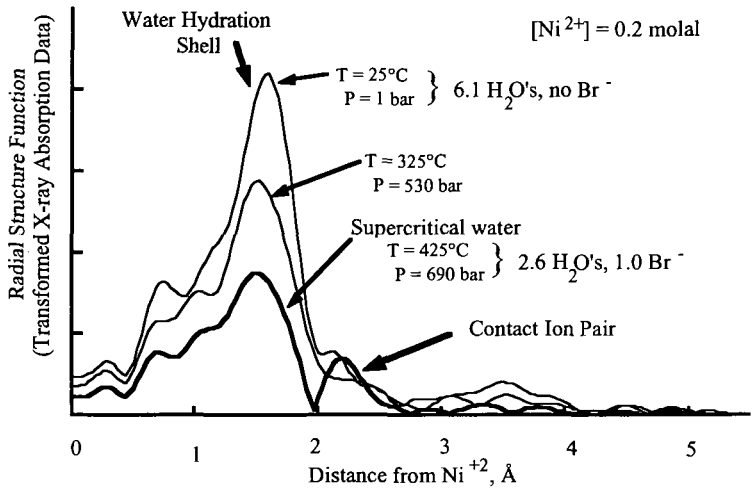

Figure 2. Radial structure around Ni^{2+} ions in supercritical water and the evolution of the Br^- contact ion pair. Distances are not corrected in this figure for the XAFS phase shift but the corrected distances are reported in the following tables.

Table 1. De-hydration of cations/anions in SC Water $[M^{n+}] = 0.2$ m

	Ambient		Supercritical			
Ion	Number of nearest waters	Distance of nearest waters	Temp. °C	Number of nearest waters	Distance of nearest waters	% De-Hydration
Rb^{1+}	5.6	2.93 Å	425	3.6	--	36%
Br^{1-}	7.1	3.35 Å	425	2.8	3.39 Å	60%
Sr^{2+}	7.3	2.60 Å	385	3.6	--	51%
Ni^{2+}	6.1	2.06 Å	425	2.6	2.095 Å	57%

Table 2. Hydration and contact-ion pair structure of Ni^{2+} in ambient, subcritical and supercritical water from Ni and Br XAFS measurements. $[NiBr_2] = 0.2$ molal , $[NaBr] = 0.8$ molal.

	Ni^{2+} Hydration / Br^{1-} Hydration[a]				$NiBr_n^{(2-n)}$ Structure		
°C	Density, g/cm^3	Number H_2O's	Distance H_2O's, Å	σ^2, x10^{-3}Å^2	Number Br^{-1}'s	Distance Br^{-1}'s, Å	σ^2, x10^{-3}Å^2
25	1.05	5.9/ 7.1	2.062/ 3.36	5.9/ 28	0.0	--	--
325	0.81	[b]---/ 4.6	[b]------/ 3.29	[b]---/ 28	1.1	2.55	11
425	0.65	1.0/ 4.3	2.091/ 3.31	3.2/ 43	3.3	2.405	12

[a] Error associated with nearest neighbor numbers is approximately ± 0.3, error associated with distance is approximately ± 0.05 Å, and error associated with σ^2 is ±0.003

[b] The Ni XAFS was not measured for this concentration.